AD-A133 528 MILLIMETER WAVE GUIDING STRUCTURES AND ANTENNAS(U) 1/1
HOUSTON UNIV TX DEPT OF ELECTRICAL ENGINEERING
S A LONG 12 SEP 83 ARO-18986.3-EL DAAG29-82-K-0074
UNCLASSIFIED F/G 9/5 NL

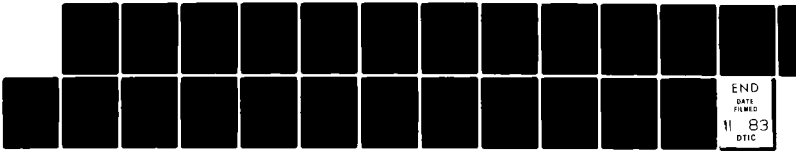

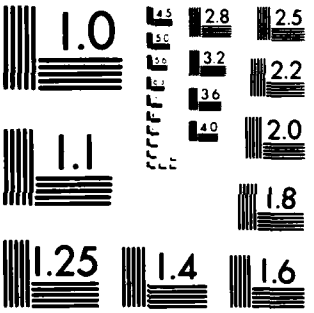

MILLIMETER WAVE GUIDING STRUCTURES AND ANTENNAS

FINAL REPORT

STUART A. LONG

September 12, 1983

U.S. ARMY RESEARCH OFFICE

Contract No. DAAG29-82-K-0074

Department of Electrical Engineering
University of Houston
Houston, Texas 77004

APPROVED FOR PUBLIC RELEASE
DISTRIBUTION UNLIMITED

Unclasified

SECURITY CLASSIFICATION OF THIS PAGE (When Data Entered)

REPORT DOCUMENTATION PAGE		READ INSTRUCTIONS BEFORE COMPLETING FORM
1. REPORT NUMBER	2. GOVT ACCESSION NO.	3. RECIPIENT'S CATALOG NUMBER
4. TITLE (and Subtitle) Millimeter Wave Guiding Structures and Antennas		5. TYPE OF REPORT & PERIOD COVERED Final Report March 1, 1982 August 31, 1983 6. PERFORMING ORG. REPORT NUMBER
7. AUTHOR(s) Stuart A. Long		8. CONTRACT OR GRANT NUMBER(s) DAAG29-82-K-0074
9. PERFORMING ORGANIZATION NAME AND ADDRESS Department of Electrical Engineering University of Houston Houston, Texas 77004		10. PROGRAM ELEMENT, PROJECT, TASK AREA & WORK UNIT NUMBERS ARO Project No. P-18986-EL
11. CONTROLLING OFFICE NAME AND ADDRESS U. S. Army Research Office Post Office Box 12211 Research Triangle Park, NC 27709		12. REPORT DATE September 12, 1983 13. NUMBER OF PAGES 22
14. MONITORING AGENCY NAME & ADDRESS(if different from Controlling Office)		15. SECURITY CLASS. (of this report) Unclassified 15a. DECLASSIFICATION/DOWNGRADING SCHEDULE

16. DISTRIBUTION STATEMENT (of this Report)

Approved for public release; distribution unlimited.

17. DISTRIBUTION STATEMENT (of the abstract entered in Block 20, if different from Report)

NA

18. SUPPLEMENTARY NOTES

THE VIEW, OPINIONS, AND/OR FINDINGS CONTAINED IN THIS REPORT ARE THOSE OF THE AUTHOR(S) AND SHOULD NOT BE CONSTRUED AS AN OFFICIAL DEPARTMENT OF THE ARMY POSITION, POLICY, OR DECISION, UNLESS SO DESIGNATED BY OTHER DOCUMENTATION.

19. KEY WORDS (Continue on reverse side if necessary and identify by block number)

Millimeter waves; antennas; dielectric resonators; dielectric antennas

20. ABSTRACT (Continue on reverse side if necessary and identify by block number)

Cylindrical, rectangular, and hemispherical resonant dielectric antennas have been investigated both experimentally and theoretically. Resonant frequencies radiation patterns, quality factors, and driving point impedance have all been measured and compared with the theoretical predictions. The structure is shown to hold promise as an efficient radiator at millimeter wave frequencies.

DD FORM 1 JAN 73 1473 EDITION OF 1 NOV 65 IS OBSOLETE

Unclassified

SECURITY CLASSIFICATION OF THIS PAGE (When Data Entered)

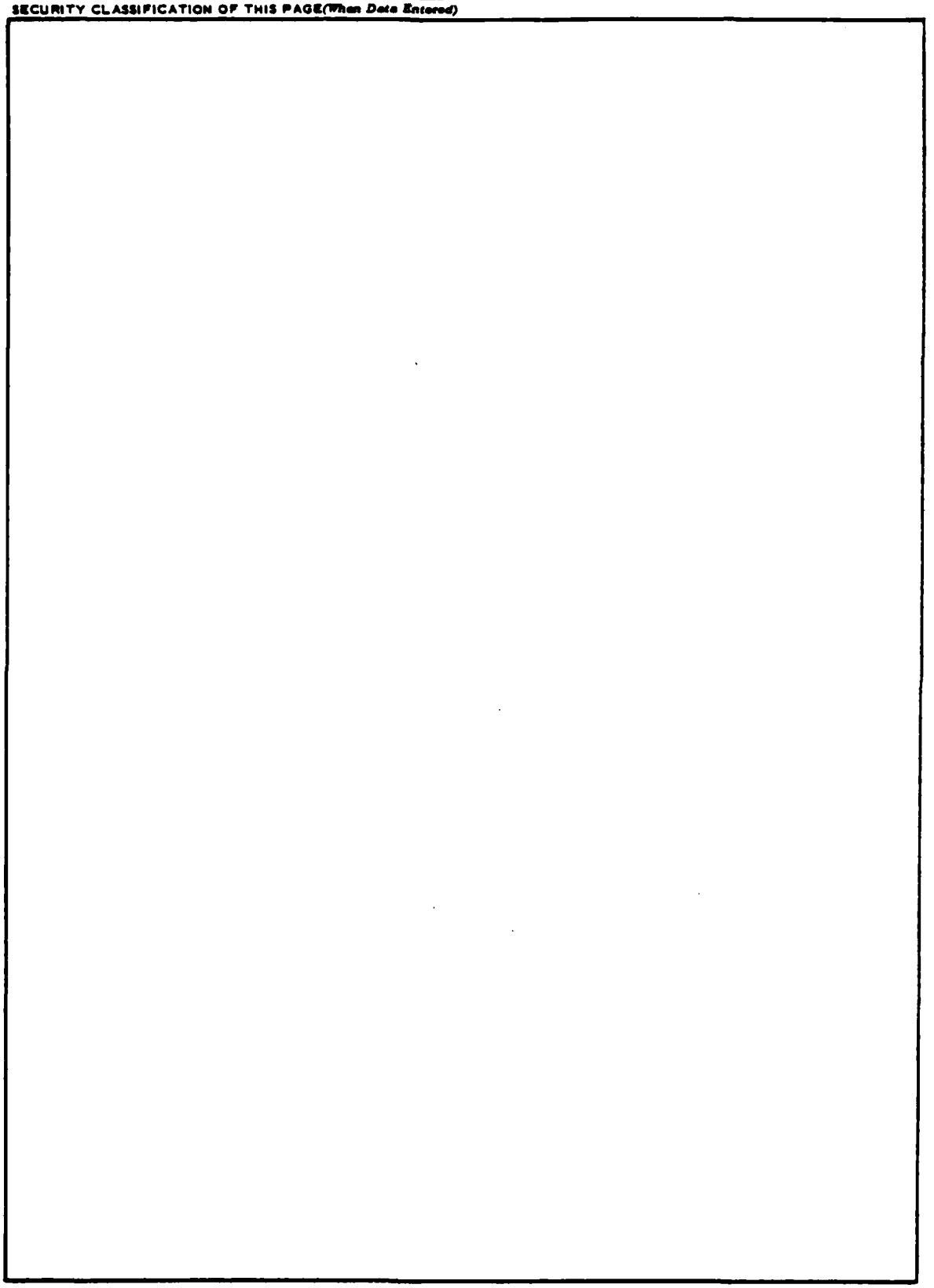

TABLE OF CONTENTS

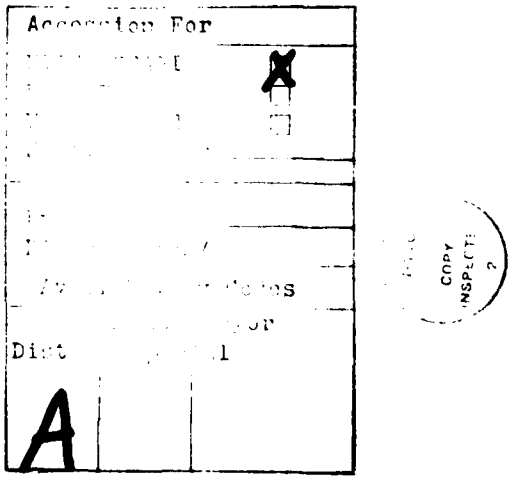

LIST OF APPENDIXES

STATEMENT OF PROBLEM

Waveguiding structures and antennas are being used presently in a wide variety of military hardware. Applications include, but are not limited to, guidance, communication, terrain sensing, fuzing, navigation, and position locating. In recent years the frequency range of interest for military systems has gradually progressed upward. For several applications today frequencies beyond the usual microwave band and in the "millimeter and near millimeter" region (100-300 GHz) are required.

Many of the waveguides and antennas that are in current use at microwave frequencies can not be simply scaled up in frequency. Conductor losses become too great for some and for others the resulting smallness in size prohibits economical fabrication. For these reasons new techinques must be developed to transport and radiate energy efficiently at these frequencies.

Typical transmission lines, such as microstrip, and guiding structures, such as rectangular conducting waveguides, can be utilized at frequencies up to 100 GHz. Beyond this point, however, conductor losses become quite high and fabrication to the required tolerances becomes exceedingly difficult. For frequencies in the 100-300 GHz range the use of dielectric waveguides seems to hold promise. A novel structure which seemingly has the possibility of radiating efficiently and allows integration with the dielectric guides is the resonant dielectric antenna. Dielectric cylinders of very high permittivity (relative dielectric contants of the order of 100-300) have been used as resonant cavities with theoretical studies previously reported.

In each case the emphasis of the investigations has been on the structure as an energy storage device, but since the cavity is not enclosed by metallic

walls, electromagnetic fields do exist beyond the geometical boundary of the cavity. Little of no work had been devoted to this structure as a radiator, nor had a complete investigation of the external fields been made. With the use of lower dielectric constant materials (5-20) and proper choices of the dimensions of the cylinder these radiation fields can be enhance and the structure be converted to an efficient radiator.

SUMMARY OF RESULTS

An antenna consisting of a piece of high-permittivity dielectric material on top of a ground plane, fed by a monopole probe extending from the ground plane into the dielectric has been investigated experimentally and theoretically. It has been shown that such a configuration will produce efficient radiation with a beam maximum normal to the ground plane if the excitation frequency was at or near the lowest resonant frequency of the dielectric. The resonant frequencies can be approximated by modelling the air-dielectric interfaces as perfect magnetic conductors.

Three basic shapes of dielectrics have been studied: cylindrical, rectangular and hemispherical. In each case is has been shown that the simplest non-azimuthally symmetric resonant mode, which was excited by a probe offset from the center of the dielectric, resulted in radiation normal to the ground plane.

The impedance of antennas with various permittivities and base dimension to height ratios have been measured. The impedance curves showed good resonant frequency agreement with the magnetic-wall model for cylindrical shapes, with modifications to the model necessary for rectangular shapes. The effects on impedance of changes in probe length, probe diameter, and probe position have also been determined.

Far-field radiation patterns, calculated using equivalent magnetic surface currents as sources, have been shown to correlate reasonable well with measurements taken in an anechoic chamber. Calculated patterns for certain higher-order modes exhibited high directive gains normal to the ground plane if the permittivity and aspect ratios were chosen correctly.

Radiation Q's have been calculated using volume currents as sources. Computation of magnetic dipole moments for the resonators were shown to give equivalent results for radiated power. The Q's thus calculated

corresponded fairly well to experimental Q's if the lower-order resonance modes are well-separated in frequency, which is the case for high width to height ratios.

The results, both theoretical and experimental, for the cylindrical resonator have been discussed in detail in Appendix A, while those for the rectangular dielectric have been included in Appendix B. An addition discussion on the external fields of the dielectric resonator and their quality factors has been summarized in Appendix C.

In conclusion the resonant dielectric antenna has been proven to be an effective radiator and should be capable of efficient operation at millimeter wave frequencies.

LIST OF PUBLICATIONS

Journal Articles

M.W. McAllister, S.A. Long, and G.L. Conway, "Rectangular Dielectric Resonator Antenna," Electronic Letters, Vol. 19, No. 6, pp. 218-219, March 17, 1983.

Abstract: An antenna which consists of a resonant rectangular parallelepiped dielectric on top of a ground plane is described. Calculated radiation patterns and measured impedances are presented, and the effects of feed probe length variations are discussed.

S.A. Long, M.W. McAllister and L.C. Shen, "The Resonant Cylindrical Dielectric Cavity Antenna," IEEE Trans. Antennas and Propagation, Vol. AP-31, pp. 406-412, May 1983.

Abstract: An experimental and theoretical investigation of the radiation and circuit properties of a resonant cylindrical dielectric cavity antenna has been undertaken. A simple theory utilizing a magnetic wall boundary condition correlates well with measured results for cylinders made from materials with larger values of dielectric constant.

Conference Presentations

Stuart A. Long and Mark W. McAllister, "An Experimental and Theoretical Investigation of the Resonant Cylindrical Dielectric Cavity Antenna," paper presented at the 1982 IEEE/AP-S International Symposium and National Radio Science Meeting, Albuquerque, NM May 1982.

Mark McAllister, Stuart A. Long and George L. Conway, "The Resonant Rectangular Dielectric Cavity Antenna," paper presented at the URSI National Radio Science Meeting, Boulder, Colorado, January 1983.

Mark McAllister and Stuart A. Long, "The Resonant Dielectric Cavity Antenna," paper presented at the 1983 IEEE Region 5 Conference, University of Houston, Houston, Texas, April 1983.

Mark W. McAllister, Stuart A. Long and George L. Conway, "The Rectangular Dielectric Resonator Antenna," paper presented at the IEEE International AP-S Symposium, University of Houston, Houston, Texas May 1983.

Stuart A. Long, M.W. McAllister, and L.C. Shen, "The Resonant Cylindrical Dielectric Antenna," paper presented at the 1983 URSI International Symposium on Electromagnetic Theory, Santiago de Compostela, Spain, August 1983.

ADVANCED DEGREES EARNED BY SCIENTIFIC PERSONNEL

Mark W. McAllister, Ph.D., Department of Electrical Engineering, University of Houston, September 1983. "The Resonant Dielectric Antenna: Experiment and Theory."

APPENDIX A

The Resonant Cylindrical Dielectric Cavity Antenna

STUART A. LONG, SENIOR MEMBER, IEEE, MARK W. McALLISTER, AND LIANG C. SHEN, SENIOR MEMBER, IEEE

***Abstract*—An experimental investigation of the radiation and circuit properties of a resonant cylindrical dielectric cavity antenna has been undertaken. The radiation patterns and input impedance have been measured for structures of various geometrical aspect ratios, dielectric constants, and sizes of coaxial feed probes. A simple theory utilizing the magnetic wall boundary condition is shown to correlate well with measured results for radiation patterns and resonant frequencies.**

I. INTRODUCTION

IN RECENT YEARS the frequency range of interest for many systems has gradually progressed upward. For applications today, frequencies beyond the usual microwave band and in the millimeter and near millimeter region (100-300 GHz) are often required. Most of the antennas that are in current use in the microwave band cannot be simply scaled up in frequency. Conduction losses in any metal portion of the radiating structure do not remain constant after scaling, and, as a result, these losses may become too great for systems requiring efficient operation. For other applications, excessive reduction in size may prohibit economical fabrication.

A novel structure which seemingly has the possibility of radiating efficiently in this frequency range is the resonant cylindrical dielectric cavity antenna. Previously dielectric cylinders of very high permittivity (relative dielectric constants of the order of 100-300) have been used as resonant cavities [1]-[6]. Theoretical studies of the dielectric cavity have been previously reported by Van Bladel [7], [8]. In each case the emphasis of the investigation has been on the structure as an energy storage device, but since the cavity is not enclosed by metallic walls, electromagnetic fields do exist beyond the geometrical boundary of the cavity. Little or no work has been devoted to this structure as a radiator, nor has a complete investigation of the external fields been made. With the use of lower dielectric constant materials ($5 \leq \epsilon_r \leq 20$), and proper choices of the dimensions of the cylinder, these radiation fields can be enhanced.

Experimental measurements have been made on several dielectric cylinders with varying geometrical aspect ratios, dielectric constants, and feed probe lengths. This work indicates that such an antenna can be designed to provide reasonably efficient radiation in the direction normal to the ground plane of the antenna. A simple theory utilizing the magnetic wall boundary condition is shown to correlate well with measured results for radiation patterns and resonant frequencies.

This type of radiator seemingly has several features which may be exploited over previously developed millimeter leaky wave antennas. Being a resonant structure, higher efficiencies may be expected, provided that suitable materials with low dielectric loss characteristics are utilized. Control of the radiated fields may also prove to be simpler with the main lobe of radiation remaining normal to the ground plane of the structure with variations in geometry and frequency. In addition, circular polarization can probably be obtained by slight changes in geometry in much the same fashion as has been previously accomplished with printed-circuit antennas [9].

Even though the emphasis of this paper is on the experimental verification of the utility of this radiating structure, the approximate theoretical analysis is presented first. The simple magnetic wall model cannot be rigorously applied for the values of dielectric constants considered. However, this method of attacking the theoretical problem provides a first order solution which is seen to provide reasonably accurate predictions for the radiation patterns and resonant frequencies. A more complicated model may be needed for other properties, such as the near field and the overall impedance, which are more sensitive to the exact field distributions.

II. THEORETICAL DERIVATIONS

A. Boundary Value Problem and Resonant Frequencies

The geometry of the problem is shown in Fig. 1 using standard cylindrical coordinates. The feed probe is temporarily ignored, i.e., the cylinder is considered uniform. Image theory can be immediately applied and the ground plane can be replaced by an imaged portion of the cylinder extending to $z = -d$; the isolated cylinder is now analyzed with an implied boundary condition of zero E_ρ and E_ϕ at $z = 0$.

An approximate solution for the fields inside such a cylinder can be obtained by assuming that the surfaces are perfect magnetic conductors. This technique has been previously justified [1]. For such a cavity, wave functions transverse electric (TE) and transverse magnetic (TM) to z may be postulated

$$\psi_{\mathrm{TE}_{npm}} = J_n\left(\frac{X_{np}}{a}\rho\right)\begin{Bmatrix}\sin n\phi\\ \cos n\phi\end{Bmatrix}\sin\left[\frac{(2m+1)\pi}{2d}\right] \tag{1}$$

$$\psi_{\mathrm{TM}_{npm}} = J_n\left(\frac{X'_{np}}{a}\rho\right)\begin{Bmatrix}\sin n\phi\\ \cos n\phi\end{Bmatrix}\cos\frac{(2m+1)\pi z}{2d} \tag{2}$$

where J_n is the Bessel function of the first kind,

$$J_n(X_{np}) = 0, J'_n(X'_{np}) = 0,$$

$$n = 1, 2, 3 \cdots, p = 1, 2, 3, \cdots, \quad m = 0, 1, 2 \cdots.$$

The separation equation $k_\rho^2 + k_z^2 = k^2 = \omega^2\mu\epsilon$ leads to an expression for the resonant frequency of the *npm* mode.

$$f_{npm} = \frac{1}{2\pi a\sqrt{\mu\epsilon}}\sqrt{\begin{Bmatrix}X_{np}^2\\ X_{np}'^2\end{Bmatrix} + \left[\frac{\pi a}{2d}(2m+1)\right]^2}. \tag{3}$$

The dominant mode is the one which has the lowest resonant fre-

Manuscript received April 5, 1982; revised September 9, 1982. This work was supported in part by the U.S. Army Research Office through the Laboratory Research Cooperative Program and under Contract DAAG29-82-K-0074.

The authors are with the Department of Electrical Engineering, Cullen College of Engineering, University of Houston, Houston, TX 77004.

0018-926X/83/0500-0406$01.00 © 1983 IEEE

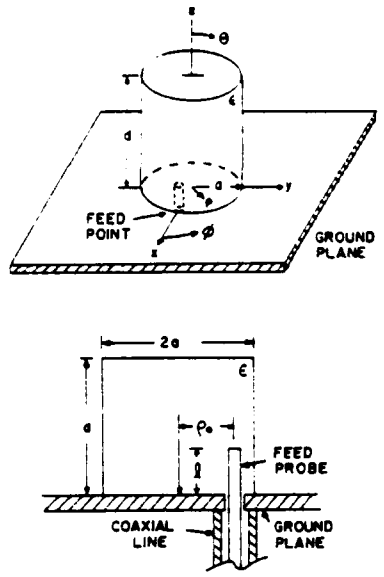

Fig. 1. Antenna geometry and feed configuration.

quency. This occurs for $m = 0, n = 1, p = 1$: $X'_{11} = 1.841$.

$$f_{dom} = \frac{1}{2\pi a\sqrt{\mu\epsilon}}\sqrt{X_{11}'^2 + \left(\frac{\pi a}{2d}\right)^2}. \tag{4}$$

B. Equivalent Magnetic Surface Currents for the Dominant Mode

The wave function of the dominant mode is

$$\psi_{TM_{110}} = \psi = J_1\left(\frac{X'_{11}\rho}{a}\right)\cos\phi\cos\frac{z\pi}{2d}. \tag{5}$$

The cos ϕ term, rather than sin ϕ, survives due to the feed position at $\phi = 0$. In anticipation of calculating the far-field patterns, tangential electric fields on the surface are determined using

$$E_\phi = \frac{1}{j\omega\epsilon\rho}\frac{\partial^2\psi}{\partial\phi\partial z}, \quad E_z = \frac{1}{j\omega\epsilon}\left(\frac{\partial^2}{\partial z^2} + k^2\right)\psi,$$

$$E_\rho = \frac{1}{j\omega\epsilon}\frac{\partial^2\psi}{\partial\rho\partial z}. \tag{6}$$

Applying $\vec{M} = \vec{E} \times \hat{n}$, where $\hat{n}$ is a unit normal pointing out of the dielectric, the following equivalent currents are found (primed coordinates are used to indicate the source).

Sides:

$$M_{z'} = \frac{\pi}{2j\omega ead}J_1(X'_{11})\sin\phi'\sin\frac{\pi z'}{2d} \tag{7}$$

and

$$M_{\phi'} = \frac{1}{j\omega\epsilon}\left(\frac{X'_{11}}{a}\right)^2 J_1(X'_{11})\cos\phi'\cos\frac{\pi z'}{2d}. \tag{8}$$

Top-bottom:

$$M_{\phi'} = \frac{\pi X'_{11}}{j2\omega ead}J'_1\left(\frac{X'_{11}\rho'}{a}\right)\cos\phi' \tag{9}$$

and

$$M_{\rho'} = \frac{\pi}{j2\omega\epsilon d\rho'}J_1\left(\frac{X'_{11}\rho'}{a}\right)\sin\phi'. \tag{10}$$

C. Calculation of Far-Field Patterns

The above currents are considered the sources for the far-field radiation. Since the radiation fields will be expressed in spherical coordinates (r, θ, ϕ), the source currents are transformed:

$$M_\theta = M_\rho\cos\theta\cos(\phi - \phi') + M_\phi\cos\theta\sin(\phi - \phi') - M_z\sin\theta \tag{11}$$

$$M_\phi = -M_\rho\sin(\phi - \phi') + M_\phi\cos(\phi - \phi'). \tag{12}$$

Electric vector potentials are then calculated:

$$F_\theta = \frac{e^{-jk_0r}}{4\pi r}\iiint M_\theta e^{jk_0[\rho'\sin\theta\cos(\phi - \phi') + z\cos\theta]}\rho'\,d\rho'\,d\phi'\,dz \tag{13}$$

$$F_\phi = \frac{e^{-jk_0r}}{4\pi r}\iiint M_\phi e^{jk_0[\rho'\sin\theta\cos(\phi - \phi') + z\cos\theta]}\rho'\,d\rho'\,d\phi'\,dz, \tag{14}$$

where $k_0 = \omega\sqrt{\mu_0\epsilon_0}$ (the free space wavenumber).

Summing the individual contributions to M_θ and M_ϕ, and integrating results in

$$F_\theta = C_1\{I_2 - I_1 - 0.5k_\rho(I_3 + I_4 - I_5 - I_6) + 1.16k_0\sin\theta J_1(k_0a\sin\theta)D_1 - 0.581k_\rho^2a \cdot [J_0(k_0a\sin\theta) + J_2(k_0a\sin\theta)]D_1\} \tag{15}$$

$$F_\phi = C_2\{-I_1 - I_2 - 0.5k_\rho(I_3 - I_4 - I_5 + I_6) - 0.581k_\rho^2a[J_0(k_0a\sin\theta) - J_2(k_0a\sin\theta)]D_1\} \tag{16}$$

where

$$C_1 = \frac{\pi^2}{j\omega\epsilon d}\frac{1}{4\pi r}\sin\phi\cos(k_0d\cos\theta)\cos\theta \tag{17}$$

$$C_2 = \frac{\pi^2}{j\omega\epsilon d}\frac{1}{4\pi r}\cos\phi\cos(k_0d\cos\theta) \tag{18}$$

$$D_1 = \left[\frac{\pi^2}{4d^2} - k_0^2\cos^2\theta\right]^{-1} \tag{19}$$

$$k_\rho = \frac{X'_{11}}{a} = \frac{1.841}{a} \tag{20}$$

$$I_1 = \int_0^a J_1(k_\rho\rho')J_0(k_0\rho'\sin\theta)\,d\rho' \tag{21}$$

$$I_2 = \int_0^a J_1(k_\rho\rho')J_2(k_0\rho'\sin\theta)\,d\rho' \tag{22}$$

$$I_3 = \int_0^a J_0(k_\rho\rho')J_0(k_0\rho'\sin\theta)\rho'\,d\rho' \tag{23}$$

$$I_4 = \int_0^a J_0(k_\rho\rho')J_2(k_0\rho'\sin\theta)\rho'\,d\rho' \tag{24}$$

$$I_5 = \int_0^a J_2(k_\rho \rho') J_0(k_0 \rho' \sin\theta) \rho' \, d\rho' \tag{25}$$

$$I_6 = \int_0^a J_2(k_\rho \rho') J_2(k_0 \rho' \sin\theta) \rho' \, d\rho'. \tag{26}$$

For the permittivities and aspect ratios under consideration ($a/d \leq 2$, $\epsilon_r \geq 5$), the term $k_0 a$ will always be less than two; this allows polynomial approximations for the above Bessel functions to be used, and the integrals are easily evaluated numerically.

In the far-field region, the electric fields are proportional to the vector potential $\vec{F}$: $E_\theta \alpha F_\phi$, and $E_\phi \alpha F_\theta$. The radiation patterns are thus found as a function of the antenna parameters.

III. THEORETICAL CALCULATIONS

The resonant frequencies as given by (3) are shown for four selected a/d ratios in Table I. The next lowest order mode after the dominant TM_{110} can either be the TM_{111} (as in the case of small a/d ratios) or the TE_{010} (for large a/d). The higher order resonances are shown for each cylinder with $\epsilon_r = 8.9$. Table II gives the resonant frequencies for several different dielectric constants for the case of $a/d = 0.5$ and $a = 0.0127$ m (a diameter of 1 in).

To illustrate the dependence of the far fields on the parameters of the antenna, several radiation patterns can be plotted. In each case the fields are shown in two principal planes. The radiated field is polarized so that it is parallel to a plane formed by a radial line from the center of base of the cylinder to the feed point and a line perpendicular to the ground plane. Since the feed is located at the $\phi = 0°$, $\rho = a$, $z = 0$ position as shown previously in Fig. 1, a graph showing E_θ versus θ for $\phi = 0, 180°$ is one principal pattern of interest. The second is that for E_ϕ at $\phi = 90°$, 270°. The major features of the radiation properties of the antenna are shown in these two patterns.

The dependence of E_θ on the shape of the cylinder (the ratio a/d) is shown in Fig. 2(a). The field is essentially omnidirectional for cylinders with larger a/d ratios. For smaller a/d ratios a null begins to develop along the direction normal to the plane of the radiator. E_ϕ in the $\phi = 90°$ plane is also shown in Fig. 2(b). A 3 dB beamwidth of 85° or greater is characteristic of the values obtained. As a/d is reduced, a dip also begins to appear in the $\theta = 0°$ direction.

IV. EXPERIMENTAL MEASUREMENTS

A. Radiation Patterns

Various dielectric materials were acquired, and cylinders were machined with different a/d ratios. One set of cylinders with various a/d ratios (see data in Table I) was made from material with $\epsilon_r = 8.9$ and mounted on a circular ground plane of diameter 7.6 cm (3 in). The sizes were chosen so that the dominant mode resonance would be near 10 GHz. Each radiator was fed by the inner conductor of a coaxial line which extended through the ground plane a distance of $l = 0.38$ cm into a hole located near the edge of the cylinder (see Fig. 1). A second set of cylinders all with $a/d = 0.5$ and $a = 0.0127$m (diameter is 1 in) was fabricated out of three different materials with $\epsilon_r = 15.2$, 6.6, and 4.5. These radiators were mounted on a 61 cm (24 in) square ground plane, were fed in a similar fashion with a longer probe of $l = 1.45$ cm, and had predicted resonances between 2.0-3.5 GHz. Far-field radiation patterns were measured in the two principal planes with the overall field linearly polarized in the $\hat{x}$ direction at $\theta = 0°$.

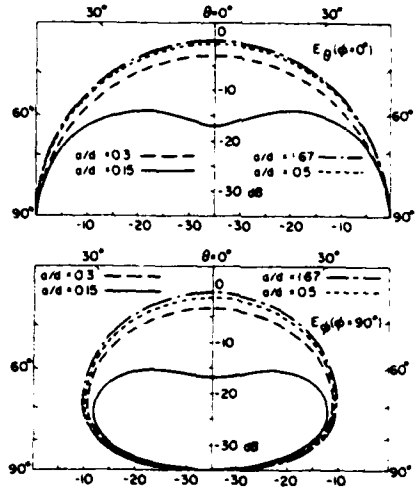

Fig. 2. Theoretical radiation patterns for various a/d ratios.

TABLE I
RESONANT FREQUENCIES (IN GHz) FOR VARIOUS a/d RATIOS ($\epsilon_r = 8.9$)

Mode	m =	0	1	2
TM_{11m}		10.13	12.38	15.95
TE_{01m}		13.07	14.88	17.97
TM_{21m}		16.48	17.96	20.58

$a/d = 0.3$, $a = 0.3$ cm; $d = 1.0$ cm, $\epsilon_r = 8.9$.

Mode	m =	0	1	2
TM_{11m}		10.67	15.95	23.14
TE_{01m}		13.49	17.97	24.57
TM_{21m}		16.82	20.58	26.54

$a/d = 0.5$, $a = 0.3$ cm; $d = 0.6$ cm, $\epsilon_r = 8.9$.

Mode	m =	0	1	2
TM_{11m}		10.24	25.82	42.32
TE_{01m}		11.38	26.29	42.60
TM_{21m}		12.48	26.98	43.03

$a/d = 1.67$, $a = 0.5$ cm; $d = 0.3$ cm, $\epsilon_r = 8.9$.

Mode	m =	0	1	2
TM_{11m}		9.90	10.53	11.66
TE_{01m}		12.89	13.38	14.29
TM_{21m}		16.35	16.72	17.46

$a/d = 0.15$, $a = 0.3$ cm; $d = 2.0$ cm; $\epsilon_r = 8.9$.

TABLE II
RESONANT FREQUENCIES (IN GHz) FOR VARIOUS DIELECTRIC CONSTANTS ($a = 0.0127$ m, $a/d = 0.5$)

Mode	$\epsilon_r = 15.2$	8.9	6.6	4.5
TM_{110}	1.93	2.52	2.93	3.55
TE_{010}	2.44	3.19	3.70	4.49
TM_{111}	2.89	3.77	4.38	5.30
TM_{210}	3.04	3.97	4.62	5.59
TE_{011}	3.25	4.24	4.93	5.97
TM_{211}	3.72	4.86	5.65	6.84

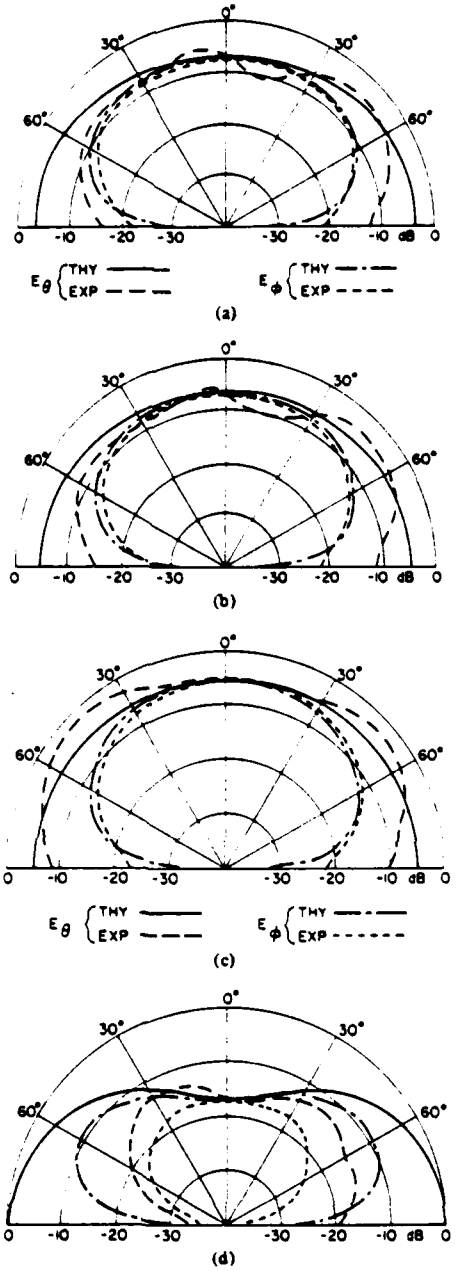

Fig. 3. Theoretical and experimental fields. (a) $a/d = 0.3$. (b) $a/d = 0.5$. (c) $a/d = 1.67$. (d) $a/d = 0.15$.

Fig. 3 illustrates the measured field patterns for the four cylinders with different values of radius-to-height ratios a/d along with the theoretically predicted fields of the past section. Reasonable agreement is found for the first three radiators. In each case the measured values of E_θ show a broad, almost omnidirectional pattern with some scalloping and a roll-off near $\theta = 90°$ (both a result of the finite ground plane used for the experimental measurements). As the a/d ratio is allowed to decrease to 0.15 for the last sample the experimental E_θ has only a dip of about 5 dB at $\theta = 0°$ as opposed to a 10 dB dip in the theory. The experimental E_ϕ shows no dip at all as compared to a theoretical one of 8 dB. It should be noted that in each case that the theoretical fields were normalized by setting the theoretical E_θ equal to the experimental value at $\theta = 0°$. All other fields shown (both E_θ and E_ϕ) are, therefore, relative to that value. When compared to a standard gain horn, a representative pattern ($a/d = 0.3$) showed an overall gain of approximately -1 dB below isotropic.

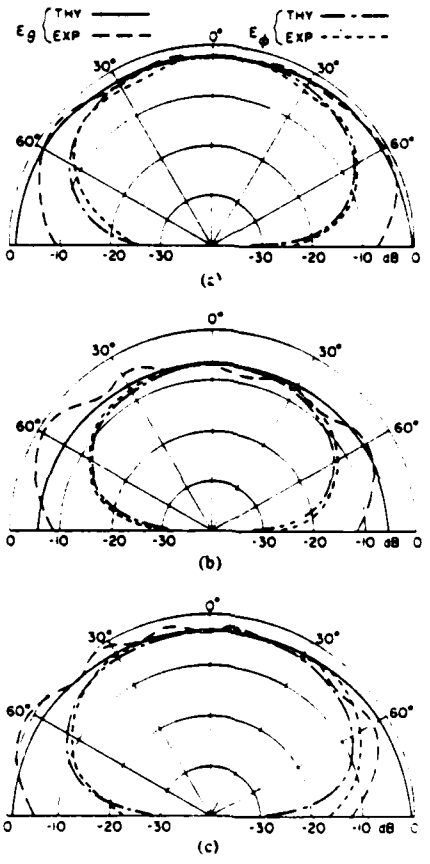

Fig. 4. Theoretical and experimental fields. (a) $\epsilon_r = 15.2$. (b) $\epsilon_r = 6.0$. (c) $\epsilon_r = 4.5$.

Fig. 4 shows the measured field patterns for the identically sized cylinders with different values of dielectric constant. Again the normalized theoretical fields are shown for comparison. Good agreement is seen again for both planes except near $\theta = 90°$ due to the finite ground plane.

B. Impedance Measurements

To determine the effects of the shape of the cylinder on the circuit characteristics of the radiator, four cylinders were fabricated with various radius-to-height ratios. Each antenna was made from the same dielectric material with $\epsilon_r = 8.9$ and fed near its edge by the center conductor of a coaxial line which extended $l = 0.38$ cm into the cylinder. The sizes were chosen so that the theoretical value of the lowest resonant frequency would be between 9.9 and 10.7 GHz. The dimensions and first resonance are shown in Table III.

The input impedance of each cylinder was measured and its magnitude and its real and imaginary parts are shown as a function of frequency in Fig. 5. Since several closely spaced modes are excited, the usual pure resonance curves are distorted somewhat. In addition, an inductive shift causes the maximum of the real part of the impedance and the zero of the imaginary part

TABLE III
ANTENNA DESIGN PARAMETERS

Sample Number	a (cm)	d (cm)	a/d	Frequency (GHz)
1	0.3	1.0	0.3	10.13
2	0.3	0.6	0.5	10.67
3	0.5	0.3	1.67	10.24
4	0.3	2.0	0.15	9.90

not to occur at exactly the same frequency. When comparing with the theoretical resonant frequencies, the point where the real part is a maximum was chosen as the experimental value. For sample 1 with $a/d = 0.3$, the first resonance occurs just above 10 GHz very near the theoretical value of 10.13 GHz. The impedance measured for sample 2 ($a/d = 0.5$) shows a resonance near 10.5 GHz as compared to the theoretical value of 10.67 GHz (an error of ~1.6 percent). Similar behavior is seen for sample 3 ($a/d = 1.67$). The resonance near 10.5 GHz is above that of the predicted 10.24 GHz (an error of ~2.5 percent). In the case of sample 4 the first two modes are seen to be very close to each other in frequency, corresponding to the predicted values of 9.90 and 10.52 GHz for the TM_{110} and TM_{111} modes. The first mode does seem to appear near 10 GHz however.

To ascertain the effect of the dielectric constant of the material used for the cylinder, more cylinders were fabricated with $a/d = 0.5$ from materials with $\epsilon_r = 15.2$, 8.9, 6.6, and 4.5, respectively. In this instance, however, the raw stock was in the form of cylindrical rods of approximately 1-in diameter ($a = 1.283$ cm). This material was cut so that $a/d = 0.5$ and the resulting cylinders were fed by probes with $l = 1.54$ cm. Owing to their larger size, the resonant frequencies were reduced into the S-band region (2–4 GHz).

The resulting real and imaginary parts of the impedance are shown as a function of frequency in Fig. 6. Once again reasonable agreement is found between theory and experiment for the first resonant frequency. For $\epsilon_r = 15.2$ the resonance near 2.0 GHz is about 3.6 percent above the predicted 1.931 GHz. For $\epsilon_r = 8.9$ the experimental value of 2.62 GHz is above the theoretical value of 2.52 GHz by four percent. The predicted value of 2.93 GHz is within one percent of the measured 2.95 GHz for $\epsilon_r = 6.6$, while for the case of $\epsilon_r = 4.5$ the experimental value of 3.45 GHz is about three percent from the theoretical 3.55 GHz.

Previous work in analyzing similar structures with much higher dielectric constants using the magnetic wall model typically have errors of approximately five to 10 percent in the prediction of the resonant frequencies. These are almost always TE modes, however, and in our case the mode of interest is a TM one. In Yee's work [1], using materials with $\epsilon_r = 100$, resonances were found to occur at frequencies corresponding to errors of less than one percent. Thus for our lower dielectric constant materials errors of two to five percent appear to be reasonable.

C. Impedance Matching

In all previous measurements the feed was located at a point near the edge of the cylinder. Since the z-directed electric field has a radial variation like $J_1(1.841\rho/a)$, it should be possible to change the impedance by shifting the position of the feed away from the edge. This technique has been previously exploited as an impedance matching technique in the case of the circular-disk

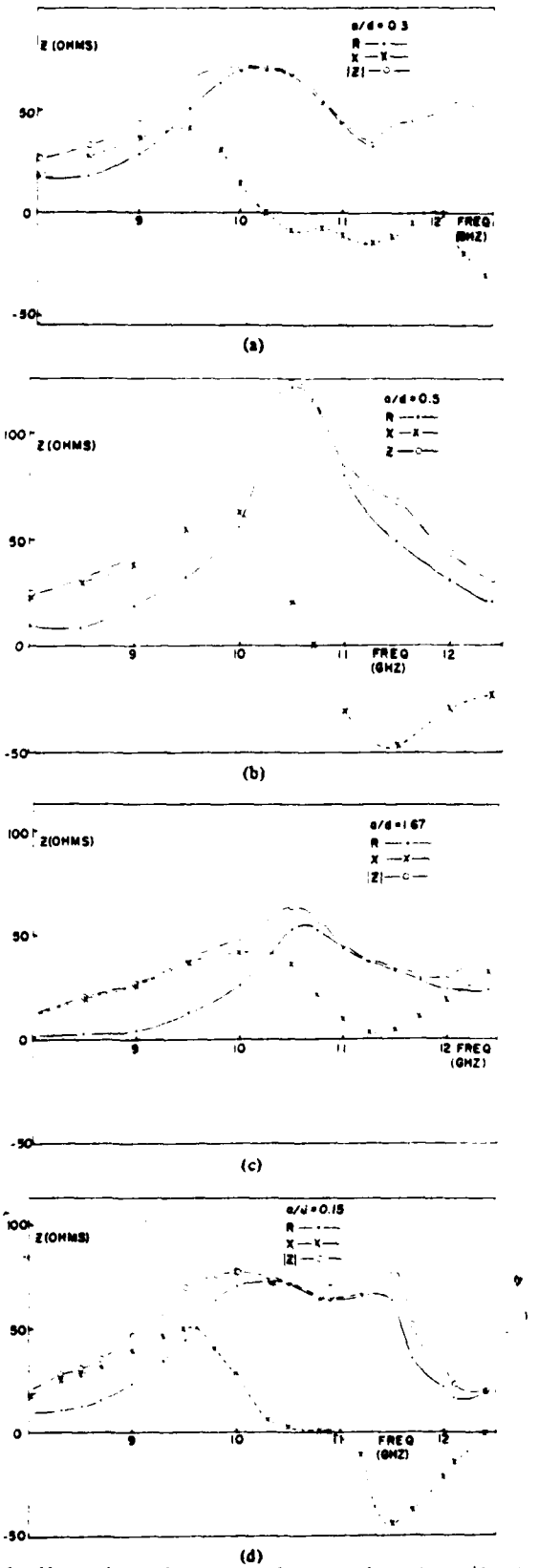

Fig. 5. Measured impedance versus frequency for various a/d ratios; $\epsilon_r = 8.9$. (a) $a/d = 0.3$. (b) $a/d = 0.5$. (c) $a/d = 1.67$. (d) $a/d = 0.15$.

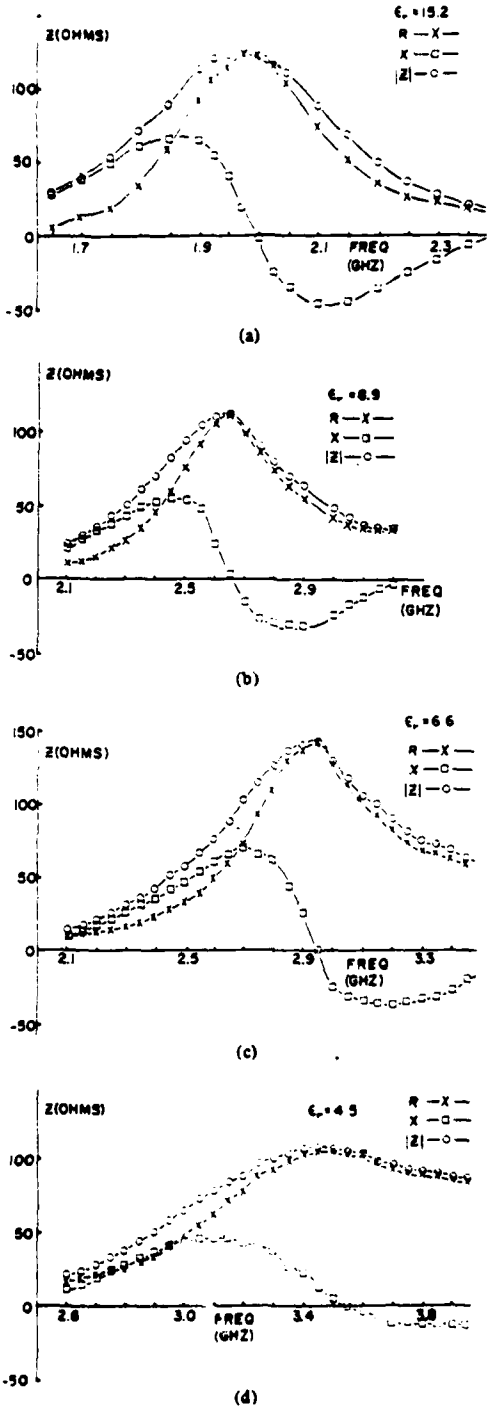

Fig. 6. Measured impedance versus frequency for various values of ϵ_r; $a/d = 0.5$. (a) $\epsilon_r = 15.2$. (b) $\epsilon_r = 8.9$. (c) $\epsilon_r = 6.6$. (d) $\epsilon_r = 4.5$.

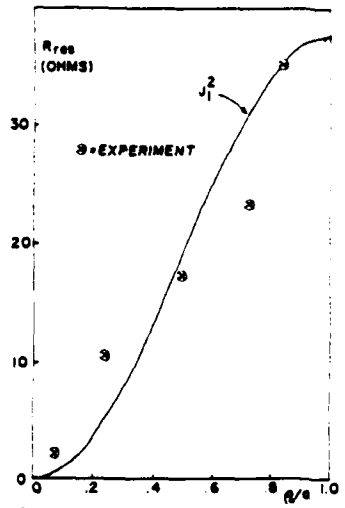

Fig. 7. Measured resistance at resonance versus radial feed point position.

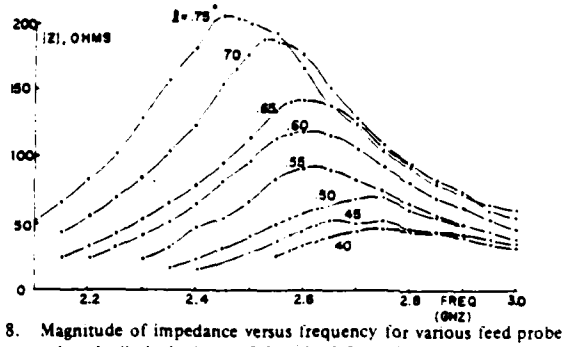

Fig. 8. Magnitude of impedance versus frequency for various feed probe lengths (in inches): $\epsilon_r = 8.9$; $a/d = 0.5$; $a = 0.0127$ m.

printed-circuit antenna [11]. As previously derived [11], the resistance at resonance resulting from the given E_z dependence on radial position gives a theoretical variation in impedance proportional to $J_1^2(k_\rho \rho_0)$ where ρ_0 is the radial coordinate of the feed position. The resistance at resonance was measured at five different feed positions for a radiator with $\epsilon_r = 15.2$ and $l = 0.38$ cm and the theory was normalized at the outermost point ($\rho_0/a = 0.83$). This theoretical curve is shown in Fig. 7 along with the five experimental values. Even though fluctuations are seen, the general behavior is verified at least in a qualitative sense.

Another matching technique which is apparent from the lower values of resistance at resonance seen in Fig. 7 is the variation in feed probe length. Impedance measurements were taken for a cylinder with $\epsilon_r = 8.9$ ($a/d = 0.5$, $a = 0.0127$ m) for feed probe lengths varying from $l = 0.40$ to 0.75 in (1.0 to 1.9 cm). The resulting magnitudes of the impedances are shown in Fig. 8 and the ability to control the resistance at resonance by varying the feed length can be seen.

It should be noted that the measured impedance behavior is really a combination of two effects—one due to the resonance associated with the dielectric cylinder and the other from the feed probe itself. The length of the feed seems to affect mainly the magnitude of the impedance at resonance while the size of the cylinder is most important in determining the resonant frequency. Any meaningful attempt to predict the actual impedance behavior theoretically must include both of these effects.

V. CONCLUSION

An introductory experimental investigation of the resonant cylindrical dielectric cavity antenna has been made. This antenna was shown to be capable of providing efficient radiation in the direction normal to its ground plane while retaining many desirable features necessary for future applications in the millimeter wave frequency region. The radiation and circuit properties were measured as a function of the physical parameters of the cylinder and reasonable correlation was found when compared with a simple theory based on a magnetic wall boundary condition.

ACKNOWLEDGMENT

The authors would like to acknowledge the aid of Fred Farrar and the other members of the microwave branch at the Harry Diamond Laboratories, Adelphi, MD, for their aid in the experimental portion of this work during the summer of 1981.

REFERENCES

[1] H. Y. Yee, "Natural resonant frequencies of microwave dielectric resonators," *IEEE Trans. Microwave Theory Tech.*, vol. MTT-13, p. 256, Mar. 1965.

[2] K. K. Chow, "On the solution and field pattern of cylindrical dielectric resonators," *IEEE Trans. Microwave Theory Tech.*, vol. MTT-14, pp. 439, Sept. 1966.

[3] S. B. Cohn, "Microwave band-pass filters containing high-Q dielectric resonators," *IEEE Trans. Microwave Theory Tech.*, vol. MTT-16, pp. 218–227, Apr. 1968.

[4] T. Itoh and R. Rudokas, "New method for computing the resonant frequencies of dielectric resonators," *IEEE Trans. Microwave Theory Tech.*, vol. MTT-25, pp. 52–55, Jan. 1977.

[5] C. Chang and T. Itoh, "Resonant characteristics of dielectric resonators for millimeter-wave integrated circuits," *Archiv für Elektronik und Übertragungstechnik*, vol. 33, pp. 141–144, Apr. 1979.

[6] P. Guillon and Y. Garault, "Accurate resonant frequencies of dielectric resonators," *IEEE Trans. Microwave Theory Tech.*, MTT-25, pp. 916–922, Nov. 1977.

[7] J. Van Bladel, "On the resonances of a dielectric resonator of very high permittivity," *IEEE Trans. Microwave Theory Tech.*, vol. MTT-23, pp. 199–208, Feb. 1975.

[8] ——, "The excitation of dielectric resonators of very high permittivity," *IEEE Trans. Microwave Theory Tech.*, vol. MTT-23, pp. 208–217, Feb. 1975.

[9] S. A. Long, L. C. Shen, D. H. Schaubert, and F. Farrar, "An experimental study of the circular polarized elliptical printed-circuit antenna," *IEEE Trans. Antennas Propagat.*, vol. AP-29, pp. 95–99, Jan. 1981.

[10] M. Abramowitz and I. Stegun, Eds., *Handbook of Mathematical Functions*, Washington, DC: Nat. Bur. Stand., 1968.

[11] S. Long, L. Shen, M. Walton, and M. Allerding, "Impedance of a circular-disc printed-circuit antenna," *Electron. Lett.*, vol. 14, no. 21, pp. 684–686, Oct. 12, 1978.

Stuart A. Long (S'65–S'72–M'74–SM'80), for a photograph and biography please see page 98 of the January 1931 issue of this TRANSACTIONS.

Mark W. McAllister, for a photograph and biography please see page 1200 of the November 1982 issue of this TRANSACTIONS.

Liang C. Shen (S'65–M'67–SM'77), for a photograph and biography please see page 94 of the January 1981 issue of this TRANSACTIONS.

RECTANGULAR DIELECTRIC RESONATOR ANTENNA

APPENDIX B

Indexing terms: Antennas, Dielectric resonators

An antenna which consists of a resonant rectangular parallelepiped dielectric on top of a ground plane is described. Calculated radiation patterns and measured impedances are presented, and the effects of feed probe length variations are discussed.

Introduction: Dielectric resonators, which have found frequent applications as microwave circuit elements, can also be useful as radiators if the shapes, permittivities and feed mechanisms are appropriately chosen. It has recently been shown[1] that a dielectric cylinder, placed on top of a ground plane and excited by a monopole probe fed from beneath the ground plane into the dielectric, will radiate efficiently in a direction normal to the ground plane when the excitation frequency is at or near the lowest resonant frequency of the cylinder. The resonances are found by modelling the cylinder as a cavity with perfect-magnetic-conductor surfaces ('magnetic-walls'). Impedance measurements on the cylinders show resonant frequencies in good agreement with the magnetic-wall model. The present work extends the above investigation to rectangular resonators.

Experimental investigation: Fig. 1 shows the antenna configuration, with the feed probe located near one of the resonator edges and centred at $y = 0$. The lowest-frequency mode excited with the probe position shown is the TM^{x}_{101} mode, where the symbols indicate one variation in the x and z directions and no variation in the y direction. This mode produces maximum radiation normal to the ground plane, as will be discussed below.

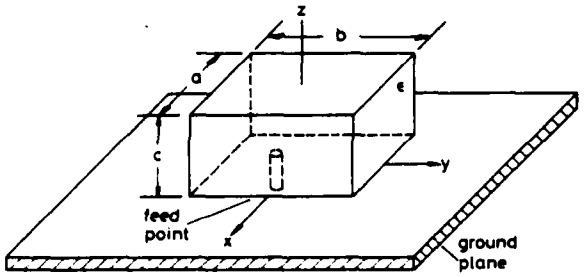

3867/1

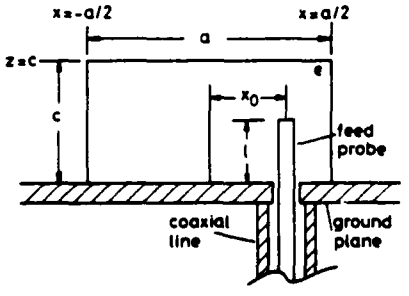

Fig. 1 *Antenna geometry and feed mechanism*

Rectangular pieces of dimension 1·5 cm × 1·5 cm × 0·75 cm were fabricated from four kinds of dielectric materials. The measured relative permittivities were 8·9, 12·8, 15·2 and 17·1. The pieces were used as building blocks in constructing antennas of various shapes. These antennas were placed on a ground plane measuring 16 cm × 16 cm, and impedance measurements were made using a network analyser.

It was found that the measured resonant frequencies did not agree as well with the predicted frequencies using a total-magnetic-wall model as did those in the cylindrical case. This corresponds with results in the literature;[2,3] for purely TM modes the magnetic-wall model is adequate, but for low-order TE adjustments are necessary. The mode investigated here is

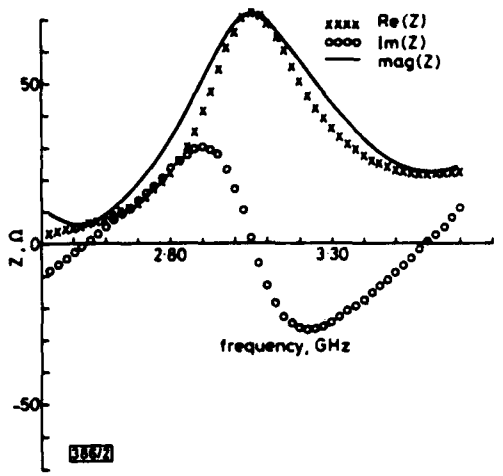

3867/2

Fig. 2 *Measured impedance*

$a = 3$ cm, $b = 1·5$ cm, $c = 1·5$ cm, probe length = 1·03 cm, $\varepsilon_r = 8·9$

TM to z but also TE to y. The adjustment consists of treating the resonator as a dielectric body inside rectangular magnetic-wall waveguide; the waveguide operates above cutoff inside the dielectric boundaries and below cutoff outside. Resonant frequencies found using this model were in better agreement with experimental data. A typical measured impedance curve is shown in Fig. 2. The predicted resonant frequency using the adjusted first-order model is 3·02 GHz.

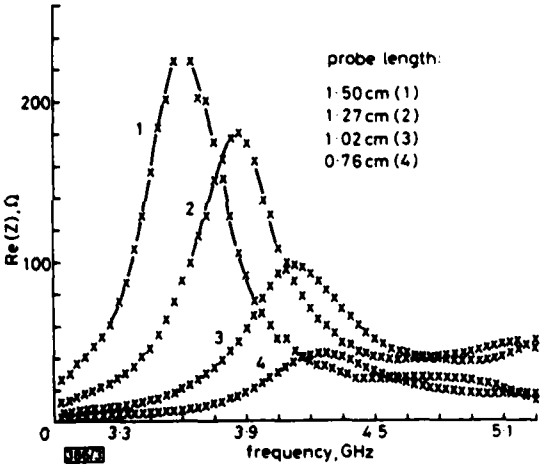

3867/3

Fig. 3 *Measured impedance with different probe lengths*

$a = b = c = 1·5$ cm, $\varepsilon_r = 8·9$

The significance of feed probe length is illustrated in Fig. 3, where the real part of the impedance is shown for different probe lengths. Monopole resonances, occurring at frequencies where the probe length is equal to a half-wavelength in the dielectric, appear to dominate when the cavity resonance is near the same frequency. A resonance for the 1·50 cm probe occurs at 3·35 GHz; the peak shown at 3·6 GHz apparently represents this. (The higher-frequency experimental peak is possibly due to the probe 'seeing' a permittivity slightly lower than that of the dielectric due to its position near the edge.) For the 0·76 cm probe the monopole resonance is above 6·6 GHz, and the peak shown at 4·2 GHz is due entirely to the cavity resonance.

Radiated fields: Radiation patterns are found by considering the tangential electric fields on the resonator surfaces as equivalent current sources for the far-field radiation. This technique gave good agreement between theory and experiment in the cylindrical case[1] and is utilised once again.

The calculated radiation patterns for square-base resonators of various heights are shown in Fig. 4. For maximum radiation normal to the ground plane, it is clear that the height of

the resonator should be less than the width. However, from a practical viewpoint the height needs to be large enough so that the probe length is greater than a quarter-wavelength in the dielectric to avoid a highly reactive impedance. Isotropicity in the θ-plane can also be improved by making the antennas longer in the x-direction or by using higher dielectric constants.

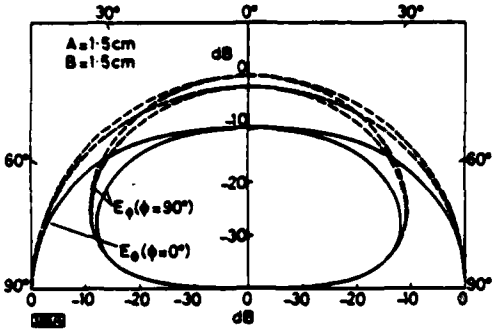

Fig. 4 *Calculated radiation patterns for square-base resonator*

c = 0·75 cm (outer), c = 2·25 cm (middle) and c = 4·50 cm (inner) for 90° and 0° curves

ε_r = 8·9

Acknowledgment: This work was supported in part by US Army Research Office Contract no. DAAG 20-82-K-0074.

M. W. McALLISTER
S. A. LONG
G. L. CONWAY

Department of Electrical Engineering
University of Houston
Houston, TX 77004, USA

7th February 1983

References

1 LONG, S. A., MCALLISTER, M. W., and SHEN, L. C.: 'The cylindrical resonant dielectric cavity antenna', *IEEE Trans.*, 1983, AP-31

2 YEE, H. Y.: 'Natural resonant frequencies of microwave dielectric resonators', *ibid.*, 1965, MTT-13, p. 256

3 OKAYA, A., and BARASH, L. F.: 'The dielectric microwave resonator', *Proc. IRE*, 1962, 50, p. 2081

0013-5194/83/060218-02$1.50/0

APPENDIX C

EXTERNAL FIELDS OF DIELECTRIC RESONATORS

Mark W. McAllister, Stuart A. Long, and Liang C. Shen
Department of Electrical Engineering
University of Houston
Houston, Texas 77004

A cylindrical dielectric slab of moderately high permittivity ($\varepsilon_r \geq 10$), placed atop a ground plane and excited by a probe internal to the dielectric (fed from beneath the ground plane), has been shown to be an efficient radiator if the excitation frequency is at or near the lowest resonant frequency of the slab [1]. The resonant frequency is calculated by treating the dielectric-air interfaces as perfect magnetic conductors.

Attempting to find the far-fields of such an antenna by using the surface fields of the dielectric as equivalent source currents in free space leads to difficulties, since the electric surface current is identically zero because of the assumed magnetic-wall boundary condition. Using the magnetic surface current as the only source leads to the wrong answers for the far-field magnitudes.

To shed light on the problem, several dielectric resonator configurations with analytical solutions are studied. These are: (a) The resonant dielectric sphere in free space, (b) the cylindrical dielectric resonator inside a radial magnetic-wall waveguide, (c) the cylindrical dielectric resonator inside a cylindrical magnetic-wall waveguide, and (d) the rectangular dielectric resonator inside a rectangular magnetic-wall waveguide.

In all cases the following procedure is used. First, expressions are derived for the source-free internal fields and the corresponding external fields. Then the dielectric is removed and new "internal" and external fields are postulated. The new fields are of the same form but have as-yet-undetermined amplitude coefficients. The tangential fields are matched at the boundary with discontinuities equal to the equivalent magnetic and electric surface currents taken from the earlier exact solutions. When both magnetic and electric surface currents are used, the new external field magnitudes are naturally found to be equal to the previous exact external field magnitudes. The next step is to neglect the electric surface current (set equal to zero), and to let the term $k_0 a$ become small, where a is the radius of the sphere or cylinder (or the length of the rectangular parallelipiped), and k_0 is the free-space wavenumber. The new external field magnitudes are recomputed and compared with the exact solutions.

The dielectric sphere is the only finite structure for which the exact external fields can be found. The surface of such a sphere resonating in a TM mode has been shown in the literature to approach a magnetic-wall boundary condition [2]. Figure 1 shows the results of carrying out the above procedure: The E_θ magnitudes are a fraction $n/(2n+1)$ of the exact values, and for E_ϕ the fraction

is (n+1)/(2n+1). Only the principal mode index n affects the answers; the indices m and p are not a factor.

A radiation Q for a magnetic-wall-modelled sphere can be found by computing external fields using only magnetic surface current as the source, then multiplying by the appropriate fraction from the graph in Figure 1. The stored energy is easily found using a cavity model. For the TM_{101} mode, the calculated Q is derived as $Q=.0055\epsilon_r^{2.5}$. This curve is shown in Figure 2, along with exact radiation Q's found by solving for the complex resonant frequencies [3].

For the cylindrical resonator "sandwiched" in a radial magnetic-wall waveguide the above procedure is more complicated since all non-azimuthally symmetric modes are hybrid HE modes: four simultaneous equations, rather than two, need to be solved. The results for an HE_{nmp} resonator are shown in Figure 3; a/d is the ratio of radius to length of the cylinder. As in the spherical case, only the principal mode index n affects the solutions, and again there is symmetry about 0.5 for the fractions representing the two different field components.

The cylindrical resonator is next placed in a cylindrical magnetic-wall waveguide. The modes of interest are $TM_{nm\delta}$, where δ is a fraction of a half-cycle in the dielectric. Figure 4 shows the results: there is still symmetry between the fractions for the two field components, as before, but now the second mode index m affects the numbers.

For the rectangular resonator in a rectangular magnetic-wall waveguide, a $TM_{nm\delta}$ mode is postulated and curves quite similar to those in Figure 4 can be obtained.

Acknowledgements

This work was supported in part by the U.S. Army Research Office through Contract DAAG29-82-K-0074.

References

[1] S.A. Long, M.W. McAllister and L.C. Shen, "The Cylindrical Resonant Dielectric Cavity Antenna," IEEE Trans. Antennas and Propagation, May 1983.

[2] J. Van Bladel, "On the Resonances of a Dielectric Resonator of Very High Permittivity," IEEE Trans. Microwave Theory and Techniques, Vol. MTT-23, February 1975.

[3] M. Gastine, L. Courtois, and J.L. Dorman, "Electromagnetic Resonances of Free Dielectric Spheres," IEEE Trans. Microwave Theory and Techniques, Vol. MTT-15, December 1967.

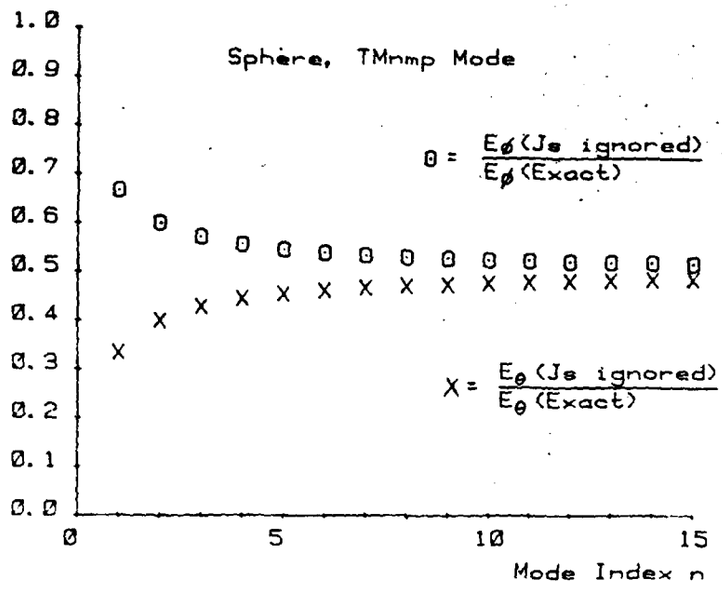

Fig. 1 Results of neglecting electric surface current in far-field calculations, dielectric sphere.

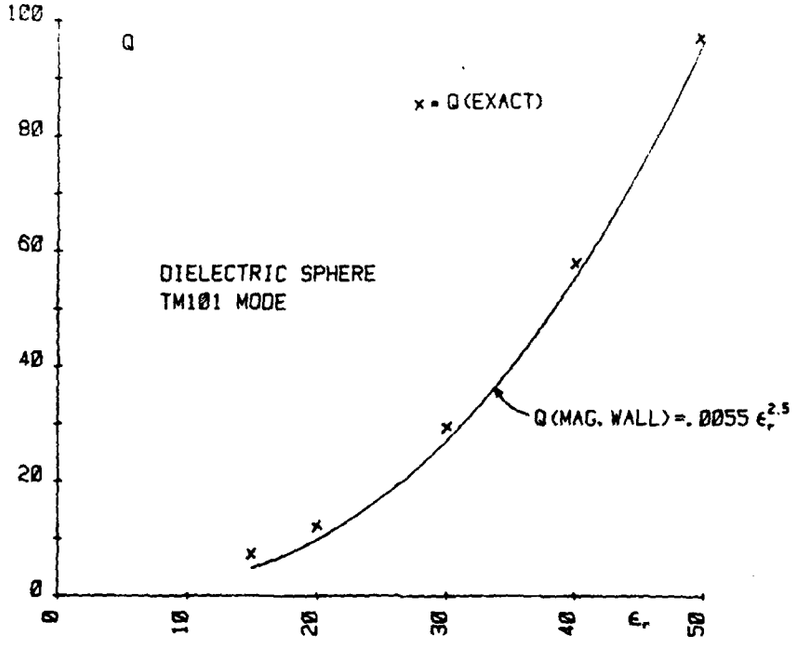

Fig. 2 Exact radiation Q vs. Q from magnetic-wall model, sphere, TM_{101} mode.

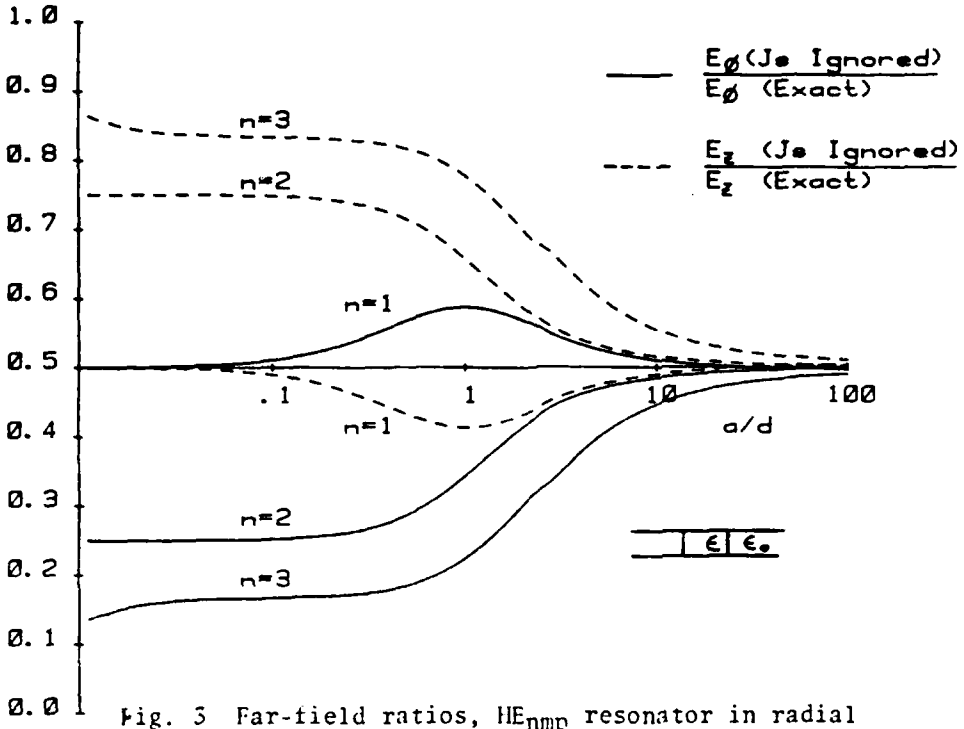

Fig. 3 Far-field ratios, HE_{nmp} resonator in radial magnetic-wall waveguide.

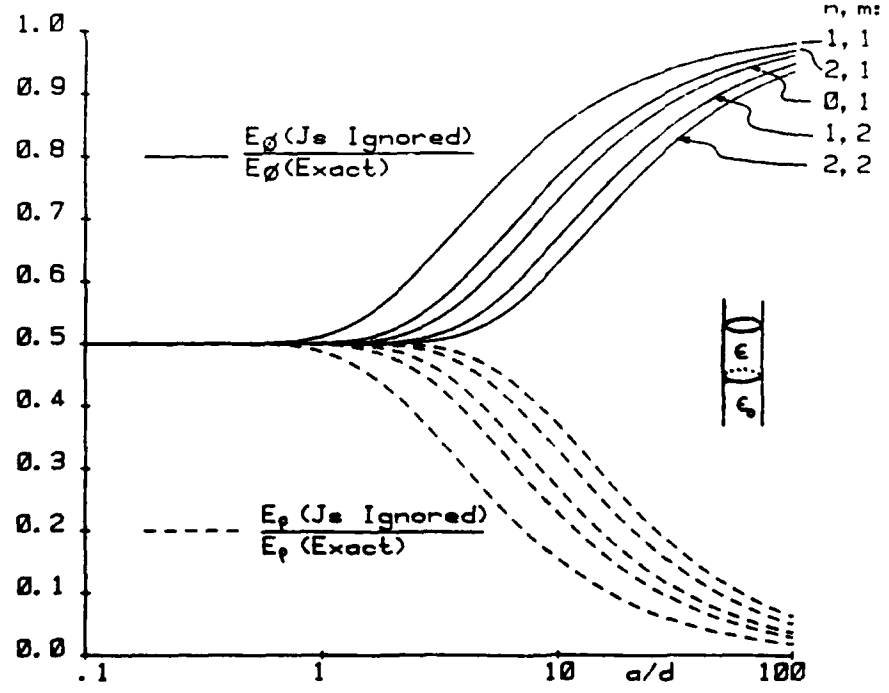

Fig. 4 Far-field ratios, $TM_{nm\delta}$ resonator in cylindrical magnetic-wall waveguide.

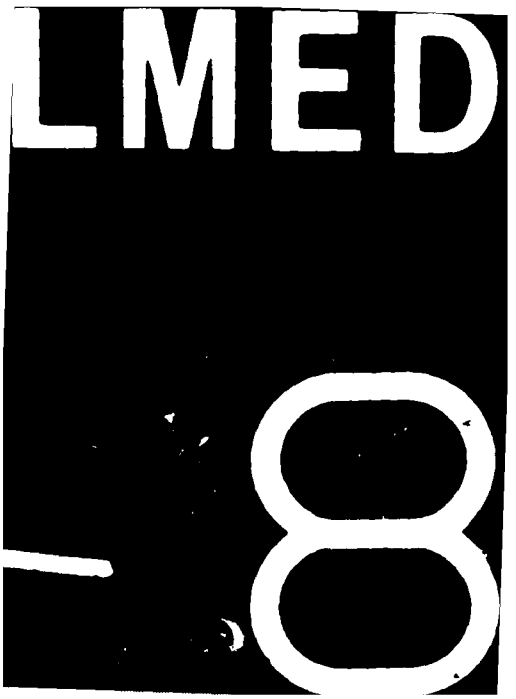
LMED
8